Universität Rostock

Traditio et Innovatio

Uncertainty Quantification for robust shape optimization of QPR

Piotr Putek[1], Shahnam Gorgi Zadeh[1],
Ursula van Rienen[1,2] Marc Wenskat[3,4]

University of Rostock,
[1]Institute of General Electrical Engineering,
[2]Department of Life, Light & Matter

[3]Universität Hamburg, Institute of Experimental Physics,
[4]Deutsches Elektronen-Synchrotron

Outline

Outline

Motivation

Reliable & predictable simulations of QPR
- Stochastic Forward Problem
- Parametrized model of QPR
- Pseudo-spectral Approach

Result for MO robust shape optimization of QPR
- Formulation of MO robust optimization
- Parameters of stochastic simulation

Conclusions

Outline

Motivation

Reliable & predictable simulations of QPR
- Stochastic Forward Problem
- Parametrized model of QPR
- Pseudo-spectral Approach

Result for MO robust shape optimization of QPR
- Formulation of MO robust optimization
- Parameters of stochastic simulation

Conclusions

Outline

Motivation

Reliable & predictable simulations of QPR

- Stochastic Forward Problem
- Parametrized model of QPR
- Pseudo-spectral Approach

Result for MO robust shape optimization of QPR

- Formulation of MO robust optimization
- Parameters of stochastic simulation

Conclusions

Uncertainties in accelerator physics

Reliable & predictable simulations of the superconducting RF resonator :

- manufacturing uncertainties : ultrasonic bath, buffered chemical polishing, etc.
  - roughness of the superconducting surfaces
  - affect the material and geometrical parameters

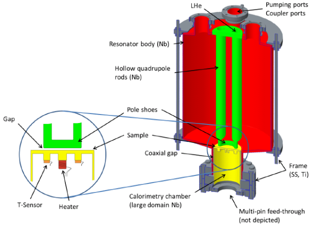

Schematic view of a HZB-QPR [K20]

Consequences of uncertainties : measurement procedure

- specifically those associated with geometrical deviations of a cavity design
- various figures of merit : a) operating frequencies – $f_0(\mathbf{p})$, b) focus factor – $f_1(\mathbf{p})$, c) homogeneity of the magnetic field distribution on the sample –$f_2(\mathbf{p})$, d) penetration of the magnetic field into the coaxial gap – $f_3(\mathbf{p})$

a) c) d)

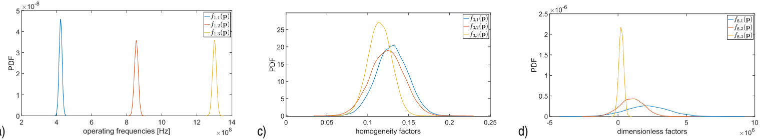

Probabilistic density functions of selected figures of merit [PGZWHvR19]

Impact of uncertainties onto optimization

Objective : robust optimization of electric devices under uncertainties

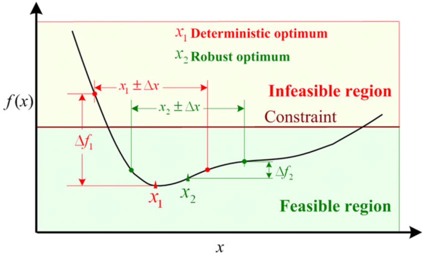

Graphical illustration of robust optimization [Wen Y. *et al.* 2011].

Stochastic Maxwell´s Eigenproblem

Eigenpairs $(\mathbf{E}(\theta), \lambda(\mathbf{p}))$:

$$
\begin{aligned}
-\nabla \times \left(\frac{1}{\mu_r} \nabla \times \mathbf{E}(\theta) \right) + \lambda\, \epsilon_r\, \mathbf{E}(\theta) &= 0, && \text{in } D,\\
\mathbf{n} \times \mathbf{E}(\theta) &= 0, && \text{on } \partial D_{\mathrm{P}},\\
\mathbf{n} \times \left(\frac{1}{\mu_r} \nabla \times \mathbf{E}(\theta) \right) &= 0, && \text{on } \partial D_{\mathrm{N}}
\end{aligned}
$$

for $\theta := (\mathbf{x}, \mathbf{p}) \in D \times \Pi$, $\partial D = \partial D_{\mathrm{P}} \cup \partial D_{\mathrm{N}}$, $\Pi \subset \mathbb{R}^Q$ - parameter space

$\mathbf{E}$: phasor of electric field, $\lambda = \frac{\omega^2}{c^2}$: eigenfrequency, ω: angular frequency

c: speed of light, μ_r: relative magnetic permeability, ϵ_r: relative electric permittivity

Discretization : finite element method

(tetrahedral mesh, piecewise linear functions)

Parametrized model of QPR

A three-dimensional symmetric model (3D)

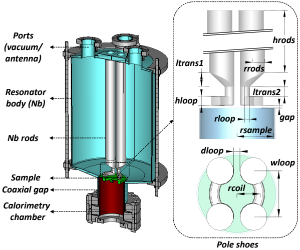

- selected parameters : $\mathbf{p}(\xi) \in \mathbb{R}^Q$, $Q = 9$

  $\mathbf{p} := (p_1, p_2, p_3, p_4, p_5, p_5, p_6, p_7, p_8, p_9)^\top :=$
  $(gap, rrods, hloop, rloop, wloop, dloop, rcoil, rsample)^\top$

  $\longrightarrow$ treated as uncertain design parameters in our simulation

UQ analysis : pseudo-spectral approach (I)

Stochastic variables (Ω, Σ, μ) : $\mathbf{p}(\xi) = (p_1(\xi), \ldots, p_Q(\xi))$, $\mathbf{p} : \Omega \to \Pi$,

independent, Gaussian, uniform, beta, etc.

Polynomial Chaos Expansion : a finite second moment of $f : [\lambda_0, \lambda_{\text{end}}]$:

$$f(\lambda, \mathbf{p}(\xi)) \doteq \sum_{i=0}^{N} v_i(\lambda)\phi_i(\mathbf{p}(\xi))$$

Based on calculations of a model at each quadrature points $\mathbf{p}^{(1)}, \ldots, \mathbf{p}^{(K)} \in \Pi$:

$$\mathbb{E}\left[f(\lambda,\ \mathbf{p})\right] = v_0(\lambda), \quad \mathrm{Var}\left[f(\lambda,\ \mathbf{p})\right] = \sum_{i=1}^{N} |v_i(\lambda)|^2$$

by using a multi-dimensional quadrature rule with weights $w^{(1)}, \ldots, w^{(K)} \in \mathbb{R}$:

$$v_i(\lambda) := \langle f(\lambda,\ \mathbf{p}),\ \phi_i(\mathbf{p})\rangle \doteq \sum_{k=1}^{K} w_k f\left(\lambda,\ \mathbf{p}^{(k)}\right)\ \phi_i(\mathbf{p}^{(k)})$$

UQ analysis : sensitivity analysis (II)

Local sensitivity :

$$\left.\frac{\partial f}{\partial p_j}\right|_{p_j=\bar{p}_j} = \sum_{i=0}^{N} v_i \frac{\partial \phi_i}{\partial p_j}\frac{\partial \mathbf{p}}{\partial \xi_j}, \quad j = 1, \dots, Q.$$

Variance-based sensitivity :

$$S_j = \frac{\mathrm{V}_j}{\mathrm{Var}(f)} \quad \text{with} \quad \mathrm{V}_j := \sum_{i \in I_j} |v_i|^2, \quad j = 1, \dots, Q,$$

I_j : sets $I_j := \{j \in \mathbb{N} : \phi_j(\mathbf{p}) \text{ is not constant in } p_j\}$

$\mathrm{Var}(f)$: the total variance, $0 \leq S_j \leq 1$: upper and lower bounds

UQ analysis of the QPR

Result for the variance-based sensitivity analysis

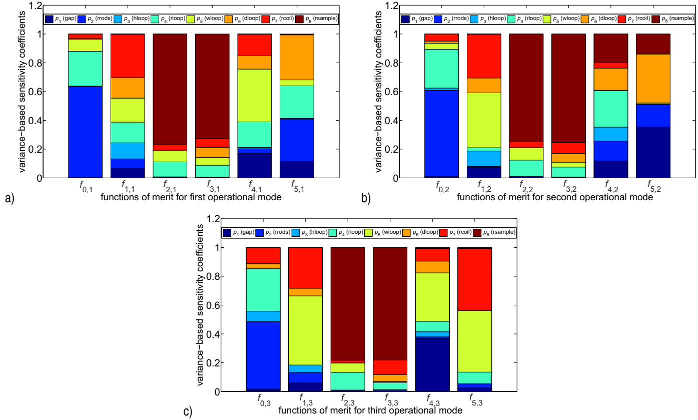

Result of the global sensitivity analysis [PGZWvR20]

Robust MO shape optimization

Random variables : $\boldsymbol{\xi} = (\xi_1, \xi_2, \xi_3, \xi_4, \xi_5)$

Random dependent functionals :

$$[f_1(\mathbf{p}), f_2(\mathbf{p}), f_3(\mathbf{p})] := \left[\frac{1}{2U} \int_{\Omega_{\mathrm{S}}} \|\mathbf{H}(\mathbf{p})\|^2 \,\mathrm{d}\mathbf{x}, \frac{\displaystyle\int_{\Omega_{\mathrm{S}}} \|\mathbf{H}(\mathbf{p})\|^2 \,\mathrm{d}\mathbf{x}}{|\Omega_{\mathrm{S}}| \max\limits_{\mathbf{x}\in\Omega_{\mathrm{S}}} (\|\mathbf{H}(\mathbf{p})\|^2)}, \frac{\displaystyle\int_{\Omega_{\mathrm{S}}} \|\mathbf{H}(\mathbf{p})\|^2 \,\mathrm{d}\mathbf{x}}{\displaystyle\int_{\Omega_{\mathrm{F}}} \|\mathbf{H}(\mathbf{p})\|^2 \,\mathrm{d}\mathbf{x}} \right]$$

Functionals for robust optimization :

$$\inf_{\overline{\mathbf{p}}\in\mathbb{R}^{\boldsymbol{Q}}} \left[\mathbb{E}(f_1), \mathbb{E}(f_2), \mathbb{E}(f_3)\right]^\top$$

$$\text{s.t. } \nabla \times (\nu \nabla \times \mathbf{E}(\mathbf{p}, \cdot)) - \lambda(\mathbf{p})\, \epsilon\, \mathbf{E}(\mathbf{p}, \cdot) = 0,$$

$$p_{L_{\boldsymbol{q}}} \leq \overline{p}_{\boldsymbol{q}} \leq p_{U_{\boldsymbol{q}}}, \text{ for } q = 1, \ldots, Q$$

Approximation of probabilistic integrals : Stroud-3 formula (10 nodes)

Parameters of stochastic simulation

Variations of geometrical parameters :

$\longrightarrow$ modeled by Gauss distribution

Random variations of parameters :

$\longrightarrow$ gap: $p_1 = \overline{p}_1(1+\delta_1\xi_1)$
$\longrightarrow$ $rrod$: $p_2 = \overline{p}_2(1+\delta_2\xi_2)$
$\longrightarrow$ $hloop$: $p_3 = \overline{p}_3(1+\delta_2\xi_3)$
$\longrightarrow$ $rloop$: $p_4 = \overline{p}_4(1+\delta_2\xi_4)$
$\longrightarrow$ $wloop$: $p_5 = \overline{p}_5(1+\delta_2\xi_5)$

- independent normal random variables : $\xi_1, \xi_2, \xi_3, \xi_4, \xi_5$
- the magnitude of perturbation : $\sigma_q := \delta_q \cdot \overline{p}_q = 0.05\,[\mathrm{mm}]$

Universität Rostock Traditio et Innovatio

Robust MO Shape Optimization : Pareto front

VBS-MO shape optimization

To solve MO robust optimization problem :

$\longrightarrow$ VBS-MO steepest descent method

$\longrightarrow$ shape derivative approximated by element-wise product : $\mathbf{S} \odot \nabla \mathbf{f}$

$\longrightarrow$ analytical expression for steepest descent direction [FS00,LR16]

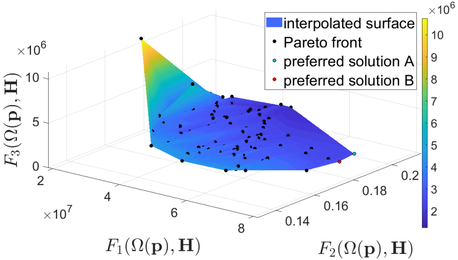

Convergence of Pareto Front using VBS-based approach [PGZWvR20]

Robust MO shape optimization: PDFs

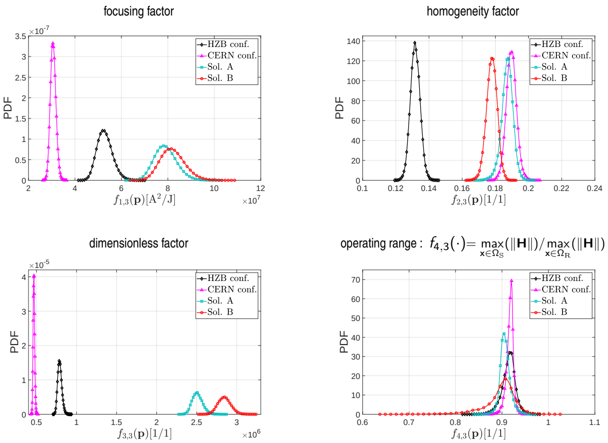

PDFs of selected figures of merit calculated in CERN-, HZB-QPR and optimized configuration [PGZWvR20]

Robust MO shape optimization

Probabilistic density functions for the frequency of the third operating mode

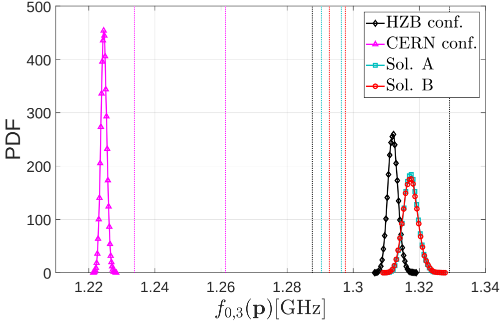

PDF of frequency for the third mode calculated in CERN -, HZB-QPR and optimized configuration [PGZWvR20]

Robust MO Shape Optimization : shapes of QPR

VBS-MO shape optimization

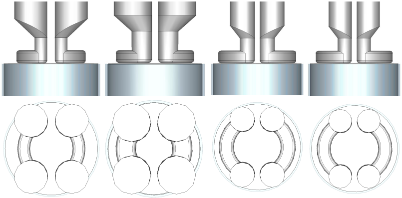

TABLE V. Results for the MO optimization – parameter domain [a]

Name		$\Omega^*_{\mathrm{HZB}}(\bar{\mathbf{p}})$	$\Omega^*_{\mathrm{CERN}}(\bar{\mathbf{p}})$	$\Omega^*_{\mathrm{A}}(\bar{\mathbf{p}})$	$\Omega^*_{\mathrm{B}}(\bar{\mathbf{p}})$
p_1 (gap)	[mm]	0.50	0.70	0.58	0.55
p_2 (rrods)	[mm]	13.00	15.00	9.76	9.14
p_3 (hloop)	[mm]	10.00	10.00	9.72	9.64
p_4 (rloop)	[mm]	5.00	8.00	5.92	5.56
p_5 (wloop)	[mm]	44.00	40.93	43.79	43.53
p_6 (dloop)	[mm]	6.00	5.00	4.00	4.00
p_7 (rcoil)	[mm]	22.408	23.00	25.00	25.00
p_8 (rsample)	[mm]	37.50	37.50	35.0	35.00

Comparison between existing QPR designs and optimized ones [PGZWvR20]

Robust MO Shape Optimization : summary

TABLE VI. Results of the MO optimization for the first mode – objective space [a]

Means/Configurations	$\Omega^*_{\mathrm{HZB}}(\overline{\mathbf{p}})$	$\Omega^*_{\mathrm{CERN}}(\overline{\mathbf{p}})$	[%]	$\Omega^*_{\mathrm{A}}(\overline{\mathbf{p}})$	[%]	$\Omega^*_{\mathrm{B}}(\overline{\mathbf{p}})$	[%]
$F_1(\Omega^*(\overline{\mathbf{p}}),\cdot)$ [M A^2/J]	50.07	32.15	-36.55	56.31	11.13	58.47	15.39
$F_2(\Omega^*(\overline{\mathbf{p}}),\cdot)$ [1/1]	0.155	0.218	41.15	0.227	48.84	0.216	39.70
$F_3(\Omega^*(\overline{\mathbf{p}}),\cdot)$ [M 1/1]	1.668	0.890	-46.64	3.941	136.3	4.421	165.1
$F_4(\Omega^*(\overline{\mathbf{p}}),\cdot)$ [1/1]	0.910	0.906	-0.43	0.901	-1.01	0.905	-0.62
$F_5(\Omega^*(\overline{\mathbf{p}}),\cdot)$ [mT/(MV/m)]	7.888	5.250	-32.93	4.824	-38.84	4.940	-37.38
$F_0(\Omega^*(\overline{\mathbf{p}}),\cdot)$ [GHz]	0.429	0.398	-7.21	0.439	2.21	0.439	2.23

[a] The columns with percentage [%] indicate a ratio (increase +/decrease -) of optimized configurations to $\Omega^*_{\mathrm{HZB}}(\overline{\mathbf{p}})$.

TABLE VIII. Results of the MO optimization for the third mode – objective space [a]

Means/Configurations	$\Omega^*_{\mathrm{HZB}}(\overline{\mathbf{p}})$	$\Omega^*_{\mathrm{CERN}}(\overline{\mathbf{p}})$	[%]	$\Omega^*_{\mathrm{A}}(\overline{\mathbf{p}})$	[%]	$\Omega^*_{\mathrm{B}}(\overline{\mathbf{p}})$	[%]
$F_1(\Omega^*(\overline{\mathbf{p}}),\cdot)$ [M A^2/J]	52.28	30.63	-42.05	78.98	49.43	82.04	55.21
$F_2(\Omega^*(\overline{\mathbf{p}}),\cdot)$ [1/1]	0.132	0.19	44.00	0.187	42.09	0.178	35.0
$F_3(\Omega^*(\overline{\mathbf{p}}),\cdot)$ [M 1/1]	0.791	0.467	-40.89	2.501	217.4	2.846	259.9
$F_4(\Omega^*(\overline{\mathbf{p}}),\cdot)$ [1/1]	0.914	0.917	0.3	0.907	-0.81	0.897	-1.94
$F_5(\Omega^*(\overline{\mathbf{p}}),\cdot)$ [mT/(MV/m)]	5.048	5.411	7.19	4.736	-6.18	4.685	-7.19
$F_0(\Omega^*(\overline{\mathbf{p}}),\cdot)$ [GHz]	1.312	1.225	-6.67	1.317	0.41	1.317	0.41

[a] The columns with percentage [%] indicate a ratio (increase +/decrease -) of optimized configurations to $\Omega^*_{\mathrm{HZB}}(\overline{\mathbf{p}})$.

Conclusions and further research

Conclusions :

⟶ VBS robust MO shape optimization problem of QPR under uncertainties

⟶ optimized configuration of QPR allows for increasing the focusing factor of the third mode by 50-57% and 158-168% compared to the HZB and CERN designs,

⟶ better resolution of the surface resistance in different $freq_i$

⟶ the dimensionless factor of $freq_3$ is more than twice bigger than for the HZB and CERN configuration

⟶ it helps to decrease the measurement bias for the third mode in HZB and CERN designs

Further research directions :

⟶ electro-stress-heat coupled problem of QPR & its optimization

Thank you for your attention